Genomic diagnostics leading to the identification of a TFG-ROS1 fusion in a child with possible atypical meningioma

Rossing, Maria; Yde, Christina Westmose; Sehested, Astrid; Østrup, Olga; Scheie, David; Dangouloff-Ros, Volodia; Geoerger, Birgit; Vassal, Gilles; Nysom, Karsten

Published in:
Cancer Genetics

DOI:
10.1016/j.cancergen.2017.03.005

Publication date:
2017

Document version
Publisher's PDF, also known as Version of record

Cancer Genetics 212-213 (2017) 32–37

Cancer Genetics

SHORT COMMUNICATION

Genomic diagnostics leading to the identification of a *TFG-ROS1* fusion in a child with possible atypical meningioma

Maria Rossing [a,*,1], Christina Westmose Yde [a,1], Astrid Sehested [b], Olga Østrup [a], David Scheie [c], Volodia Dangouloff-Ros [d], Birgit Geoerger [e], Gilles Vassal [e], Karsten Nysom [b]

[a] *Center for Genomic Medicine, Rigshospitalet, Copenhagen University Hospital, Copenhagen, Denmark;* [b] *Department of Paediatrics and Adolescent Medicine, Neuroscience Center, Rigshospitalet, Copenhagen University Hospital, Copenhagen, Denmark;* [c] *Department of Pathology, Neuroscience Center, Rigshospitalet, Copenhagen University Hospital, Copenhagen, Denmark;* [d] *Pediatric Imaging Unit, Hôpital Necker-Enfants Malades, Paris, France;* [e] *Department of Paediatrics and Adolescent Oncology, Vectorology and Anticancer Therapies, UMR 8203, CNRS, Univ. Paris-Sud, Gustave Roussy, Université Paris-Saclay, Villejuif, France*

Meningiomas are rare in children. They are highly complex, harboring unique clinical and pathological characteristics, and many occur in patients with neurofibromatosis type 2. Hereby, we present a case of a two-year-old boy presented with a diagnostically challenging intraventricular tumor. It was incompletely resected 6 times over 14 months but kept progressing and was ultimately deemed unresectable. Histologically, the tumor was initially classified as schwannoma, but extensive international review concluded it was most likely an atypical meningioma, WHO grade II. Comprehensive genomic profiling revealed a *TFG-ROS1* fusion, suggesting that ROS1-signaling pathway alterations were driving the tumor growth. In light of this new information, the possibility of a diagnosis of inflammatory myofibroblastic tumor was considered; however the histopathological results were not conclusive. This specific molecular finding allowed the potential use of precision medicine and the patient was enrolled in the AcSé phase 2 trial with crizotinib (NCT02034981), leading to a prolonged partial tumor response which is persisting since 14 months. This case highlights the value of precision cancer medicine in children.

Keywords *TFG-ROS1*, fusion gene, pediatric mesenchymal tumor, meningioma, crizotinib

Introduction

Meningiomas are rare neoplasms in children and adolescents and accounts for <5% of all pediatric brain tumors (1,2). Meningiomas in children differ from the meningioma in adults; they have male predominance, variable locations, sometimes cystic components and a poorer prognosis (3–5). Pediatric meningiomas are associated with genetic predisposing syndromes such as neurofibromatosis type 2 (NF-2) (6,7). The World Health Organization (WHO) histopathological classification of meningiomas is the same for children and adults (8). However, unlike meningiomas in adults, pediatric meningiomas are highly challenging to diagnose; up to one third are classified as atypical, and meningeal-based neoplasms have a number of differential diagnoses, e.g. sarcoma, chondroma, leukemic mass, neurocutaneous melanosis and medulloblastoma (8–10).

Due to recent large-scale sequencing efforts, the biology of adult meningiomas is currently being unraveled. The genomic alterations comprise point mutations in *NF2*, *TRAF7*, *KLF4*, *AKT1*, *SOM*, *CDKN2A7C*, *SMARCE1* and *TERT*, as well as structural variations, genomic rearrangements and

Received January 24, 2017; received in revised form March 14, 2017; accepted March 18, 2017.

* Corresponding author.
E-mail address: caroline.maria.rossing@regionh.dk

[1] Equal contribution.

http://dx.doi.org/10.1016/j.cancergen.2017.03.005

epigenetic modifications (11,12). Identification of activating oncogenes and the subsequent activation of downstream signaling pathways enable the use of targeted treatment. An early report of the implications of specific oncogenic drivers in meningiomas revealed an overexpression of *ROS1* (c-ros oncogene 1) in more than half of 31 tumors (13). ROS1 is an essential transmembrane receptor protein tyrosine kinase, regulating several cellular processes including proliferation, differentiation, apoptosis and cell migration (14). Substantial evidence supports *ROS1* as a key player in many solid tumors, especially due to *ROS1* rearrangements leading to constitutive activation of the tyrosine kinase (15,16). Crizotinib, a protein kinase inhibitor originally developed as an *ALK* inhibitor, is registered for both *ALK* and ROS1 gene rearrangements in non-small cell lung cancer (17). *ROS1* displays sequence homology with the primary structure of *ALK* and crizotinib is inhibiting ROS1 phosphorylation at a low nM range, thus supporting the rationale for crizotinib treatment of tumors driven by ROS1.

Although *ROS1* is overexpressed in half of the adult meningiomas, the role of *ROS1* in the pathogenesis of meningioma is still controversial. Furthermore, the mode of action of ROS1 in intracranial tumorigenesis is still not clarified. Nevertheless, the finding of a *ROS1*-fusion in a presumptive pediatric meningioma indicates the importance of ROS1 and substantiates its role as a treatment target in the era of precision medicine.

Patient and methods

Patient case

A 21-month-old boy presented with delayed motor development since birth, loss of motor function for three months, hypotonia and increasing head circumference. Magnetic resonance imaging (MRI) showed a large intraventricular tumor measuring $5.5 \times 6.5 \times 5.5$ cm with severe hydrocephalus (Figure 1a). The tumor was solid and contrast-enhancing. The tumor was partially resected and histology initially classified it as cellular schwannoma, WHO grade I. A ventriculoperitoneal shunt was inserted and the patient received substitution therapy for pituitary insufficiency (vasopressin, thyroid hormone and hydrocortisone). Eight and 16 months after the initial tumor surgery, the tumor was again partially resected due to residual tumor progression. Six months after the third incomplete resection, the tumor again progressed on MRI and the boy started treatment with vinblastine weekly for approximately one year. During this, the tumor kept progressing and was incompletely resected twice more. Subsequent MRIs showed continuous slow progression of residual tumors as well as new lesions occurring within the tumor cavity. Radiotherapy was considered but found inappropriate due to the very large centrally located supratentorial field. Methylation array testing suggested the tumor best resembled a subependymal giant cell astrocytoma (SEGA), but the tumor kept progressing after three months of everolimus therapy.

Histopathological diagnosis

The tumor was composed of compact sheets of spindled and focally epithelioid cells (Figure 1b). Vague whorls were encountered. The nuclei had delicate chromatin and occasional pseudo-inclusions. There were foci with lymphoplasmacytic inflammation and infiltration of brain tissue. Mitoses were few, although some foci with six mitoses per 10 high power fields were demonstrated. Foci of tumor necrosis were encountered. Immunohistochemistry revealed positive staining for vimentin and patchy staining for S-100 and EMA. Scattered tumor cells also stained for GFAP and desmin. There was no staining for cytokeratin, somatostatin receptor 2A, progesterone receptor, sox10, olig2, map2, transthyretin, synaptophysin, chromogranin, neu-n, neurofilament, collagen IV, myf4, actin, SMMS1, IDH1, CD99 and HMB45, and INI1 was normal. Ki67 staining varied between 5 and 12% and electron microscopy revealed scattered desmosomes. The histology was similar in all specimens from the consecutive resections. Several diagnoses were considered, including schwannoma and ependymoma, but results from the 450k methylation analysis were not compatible with meningioma, ependymoma or schwannoma, suggesting a plausible relation to SEGA. Subsequently, two external histopathological reviewers supported the most likely diagnosis being atypical meningioma, WHO grade II. However, recent histopathological revision raised the possibility of a tentative diagnosis of inflammatory myofibroblastic tumor (IMT), based on the inflammatory background, the partially spindled cells, as well as scattered desmin positivity. Still the widespread S-100 staining was unusual and not entirely supportive of IMT characteristics.

Genomic profiling of tumor biopsy

DNA and RNA were purified from tumor tissue from the third resection preserved in RNALater (Life Technologies) using total AllPrep DNA/RNA purification kit (Qiagen). For whole-exome-sequencing (WES), DNA libraries were prepared by fragmentation on Covaris S2 (Agilent) and adaptor ligation using KAPA HTP Library Preparation Kit. Exomes were enriched with SureSelectXT Clinical Research Exome kit (Agilent). WES was performed as paired-end sequencing using the HiSeq2500 platform from Illumina. RNA-sequencing was done using TruSeq Stranded Total RNA Library Prep Kit, and RNA was sequenced on a NextSeq500 (Illumina). Raw sequencing data from the Illumina sequencing platforms were processed with CASAVA-1.8.2. Generated fastq files were analyzed in CLC Biomedical Genomics Workbench (Qiagen) and Ingenuity Variant Analysis (Qiagen). FusionMap bioinformatics tool (Array Suite) was used for screening of fusion transcripts (18).

Microarray analysis

CytoScan assay (Affymetrix) was performed on DNA from fresh-frozen specimen achieved by tumor biopsy, according to the manufacturer's instructions. CEL files from CytoScan assay were imported into NEXUS (BioDiscovery) and used for the analysis and visualization of copy number aberrations (CNAs) and loss-of-heterogeneity (LOH). CNAs (loss, gain, biallelic loss or high amplification) and LOH calls for each sample were confirmed by visual inspection and followed by manual interpretation of whole genome profiles. In general, presence of numerical and segmental aberrations was assigned for each chromosome. CEL files are available at the ArrayExpress database under accession numbers E-GEOD-4780 and E-MTAB-1852. RNA isolated as described above

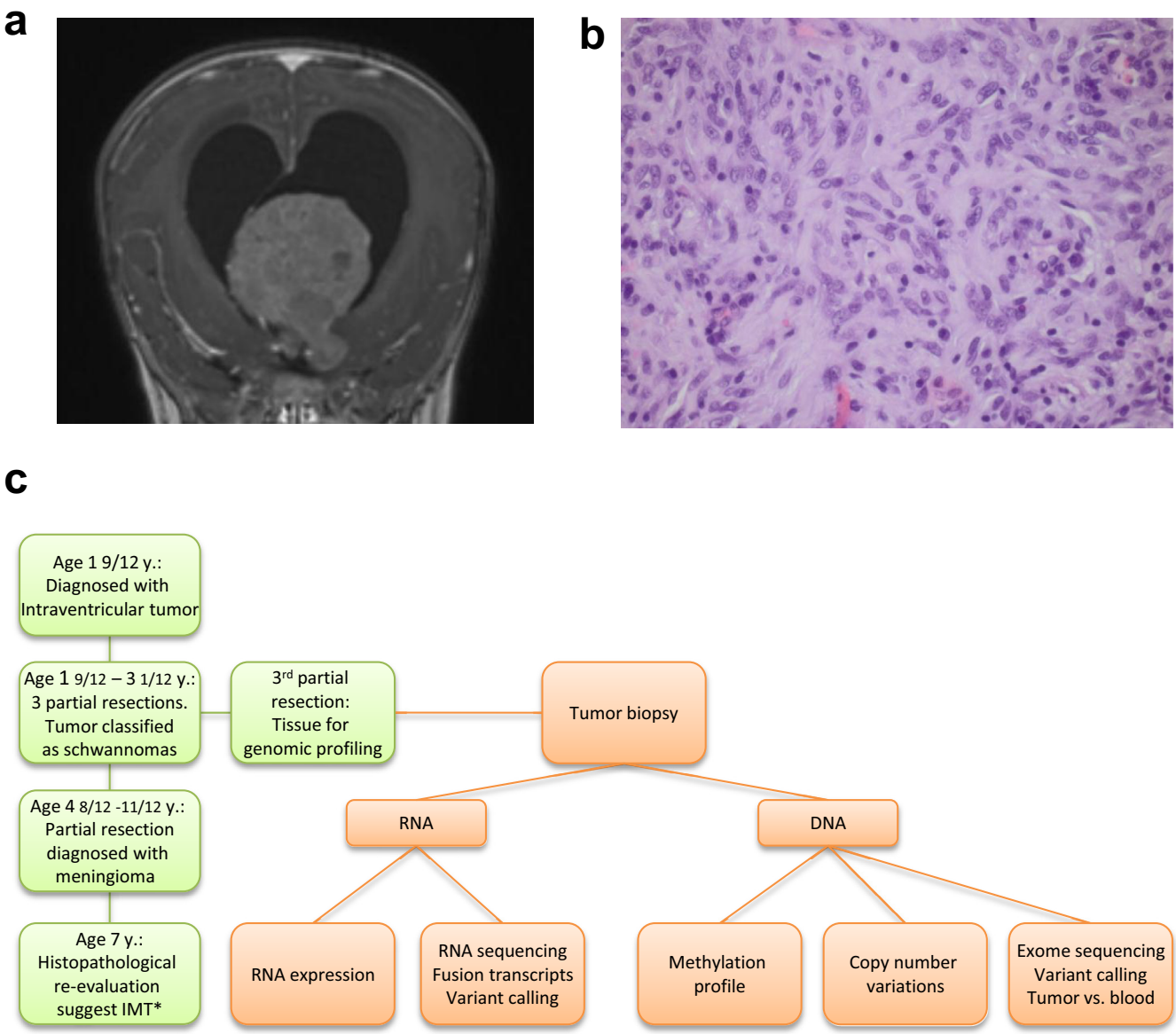

Figure 1 Diagnosis and comprehensive genomic profile of a pediatric meningioma patient**.** (a) Initial coronal MRI (T1 weighted sequence with intravenous contrast) demonstrating the tumor (5.5 × 6.5 × 5.5 cm) originating in the 3rd ventricle and extending into the left lateral ventricle, causing hydrocephalus. (b) The tumor was composed of compact sheets of spindled cells. Scattered lymphocytes were encountered. (c) Schematic outline of clinical course and comprehensive genomic profiling of tumor sample. Types of analysis performed on the tumor biopsy as part of the genomic profiling include expression array analysis, RNA-sequencing, 450k methylation array and SNP analysis and whole-exome-sequencing. IMT*, inflammatory myofibroblastic tumor.

was reverse transcribed and used for cRNA synthesis, labeling and hybridization with Human Genome U133 Plus 2.0 Array (Affymetrix) according to the manufacturer standard protocol available at www.affymetrix.com. Briefly, the arrays were washed and stained with phycoerythrin conjugated streptavidin using the Affymetrix Fluidics Station 450, and the arrays were scanned in the Affymetrix GeneArray 3000 7G scanner to generate fluorescent images. Cell intensity files (.CEL files) were generated in the GeneChip Command Console Software (AGCC; Affymetrix). Raw intensity .CEL files were preprocessed by quantile normalization, and gene summaries were extracted via robust multi-array average (19) within the Qlucore Omics Explorer™ software. Expression values for the genes were derived as an average of probe set for the particular gene. Data were randomized using permutation. Difference in the *ROS1* gene expression between the patient sample and the external data sets was determined by t-test.

Sanger sequencing/primers

The fusion breakpoint was verified by RT-PCR performed using a forward primer located in exon 5 of *TGF* (5′-GGTAGGGAAGAAAAGTCTGC-3′) and a reverse primer

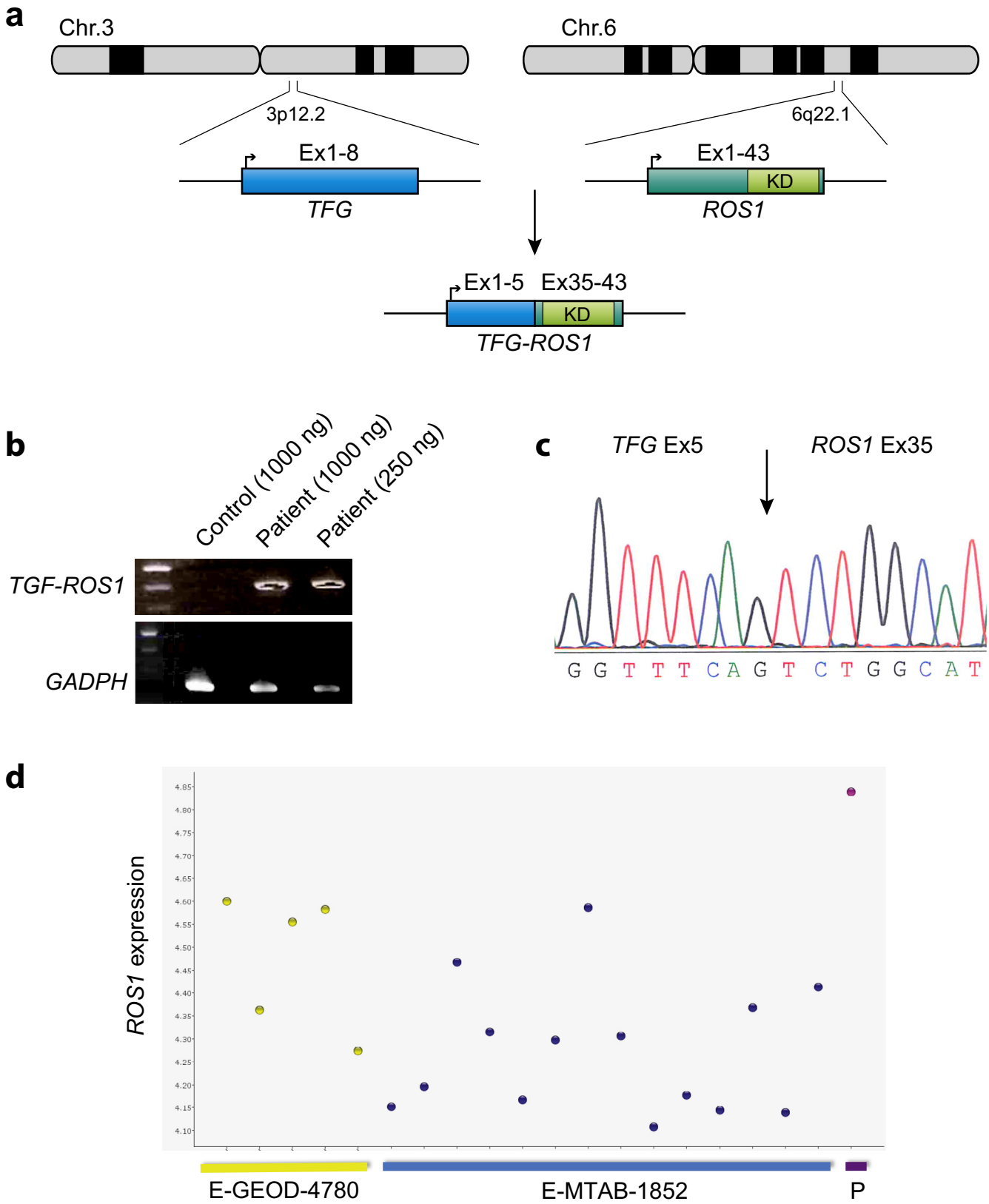

Figure 2 Identification of *TFG:ROS1* fusion. (a) RNA sequencing of a tumor biopsy from the patient revealed a fusion between *TFG* (exon 5) and *ROS1* (exon 35) resulting from a translocation at chromosomal regions 3p12.2 and 6q22.1. (b) The fusion breakpoint was validated by RT-PCR using a forward primer located in *TGF* and a reverse primer located in *ROS1* as described in the Patient and methods section. (c) The resulting RT-PCR product was subjected to Sanger sequencing**.** (d) Scatter plot showing normalized expression values of *ROS1* transcript in patient sample (violet) and in two independent data sets comprising meningioma. E-GEOD-4780 is marked yellow and E-MTAB-1852 is marked blue. KD, kinase domain; P, patient sample. (For interpretation of the references to color in this figure legend, the reader is referred to the web version of this article.)

located in exon 35 of *ROS1* (5′-TCCACTTCCCAGCAAGAGACG-3′). The RT-PCR product was sequenced by Sanger sequencing using an ABI 3730 DNA Analyzer according to the manufacturer's instructions (Applied Biosystems).

Results and discussion

Here we present the case of a 21-month-old boy with a large intracranial tumor (Figure 1a), that was diagnostically challenging. Due to the fact that complete tumor resection was not possible and standard treatment options were exhausted, recurrent tumor biopsies were subjected to comprehensive genomic profiling, consisting of exome-sequencing, SNP array, expression array and RNA-sequencing (Figure 1c). It revealed that the most likely oncogenic driver of this unique pediatric tumor was a *TFG:ROS1* fusion. Analysis of two different tumor specimens, obtained by surgeries two years apart, identified the same *TFG:ROS1* fusion in both samples (data not shown). The chromosomal rearrangement was identified between regions 3p12.2 and 6q22.1, causing fusion between exon 5 of *TFG* and exon 35 of *ROS1* (Figure 2a–c). This is in line with previous reports on *TFG:ROS1* fusions, where breakpoints were located between exon 4 of *TFG* and exon 34 or 35 of *ROS1*, resulting in the expression of a constitutively active ROS1 containing its complete kinase domain (20,21). Notably, one of the cases described was an 8-year-old boy diagnosed with treatment-refractory inflammatory myofibroblastic tumor with a *TFG:ROS1* fusion, showing a dramatic response to crizotinib (21). We compared *ROS1* expression in our tumor sample with a series of online available expression profiles from adult meningiomas (Figure 2d). As depicted in the scatter plot, *ROS1* was overexpressed in our tumor sample ($p = 0.008$; $q = 0.08$), supporting the assumption that the fusion causes overexpression. This suggests that ROS1 signaling pathways are activated and drive tumor proliferation. The fusion identified in our patient does not seem to be a frequent driver of adult meningiomas; none of the sequencing data on meningiomas available online showed a similar level of overexpression. This leads us to speculate if the tumor represented an unusual case of IMT and questioned if the diagnosis of atypical meningioma was correct for our patient. Perhaps atypical meningiomas in children are a distinct entity partially resembling histopathological features of adult meningiomas. Results from WES did not reveal any additional information regarding specific oncogenic drivers or actionable target mutations. SNP-array analysis showed no numeric or segmental alterations. In particular, ALK expression was not significantly altered, nor were there any mutations or rearrangements in *ALK*.

The role of ROS1 in meningioma is complex and only one report identified *ROS1* as being overexpressed in half of a series of adult meningiomas (13). Recent technical advances allow a broad comprehensive examination in order to identify relevant treatment targets in this rare pediatric entity, which can be crucial for the clinical course. In agreement with this, a *BRAF* V600E mutation was identified in a rhabdoid meningioma in a 6-year-old girl, who showed good clinical response to the BRAF inhibitor dabrafenib (22).

Based on the identification of the fusion transcript in his tumor, our patient was enrolled in the AcSé crizotinib trial (NCT02034981) running in France. This is a phase II basket trial exploring the activity of crizotinib in malignancies with ALK, ROS or MET alterations, other than ALK+ non-small cell lung cancer, in children, adolescents and adults with advanced relapsed or refractory disease (23). He has now been treated with oral—crizotinib (215 mg/m^2 twice daily) for 14 months with an excellent tolerance and one dose reduction after 4 cycles due to non-symptomatic G3 QTc prolongation. Two months after starting therapy, MRI showed a partial tumor response with a residual lesion, which was confirmed on all subsequent scans. This case illustrates the rationale of extensive molecular profiling of very high risk, relapsing or progressing tumors in order to identify genetic alterations driving tumor growth. Such precision cancer diagnostics enable clinicians to access and use potentially potent targeted therapy for patients not cured by current standard therapies.

Acknowledgments

We are very grateful to Dr. David Capper and the team at DKFZ, Institute of Neuropathology, University Hospital Heidelberg, Germany, for methylation array analysis and indeed to both Prof. Dr. Werner Paulus, Institute of Neuropathology, University of Münster, and Prof. Dr. Arie Perry, The Department of Pathology at the University of California, San Francisco, USA, for histopathological review. We thank Vibeke Blåbjerg and Miriam Yan Juk Guo for excellent laboratory assistance. The AcSé crizotinib trial is sponsored by Unicancer with support by the French National Cancer Institute (INCa) and Fondation ARC.

References

1. Greene S, Nair N, Ojemann JG, et al. Meningiomas in children. Pediatr Neurosurg 2008;44:9–13.
2. Tufan K, Dogulu F, Kurt G, et al. Intracranial meningiomas of childhood and adolescence. Pediatr Neurosurg 2005;41:1–7.
3. Arivazhagan A, Devi BI, Kolluri SV, et al. Pediatric intracranial meningiomas—do they differ from their counterparts in adults? Pediatr Neurosurg 2008;44:43–48.
4. Baumgartner JE, Sorenson JM. Meningioma in the pediatric population. J Neurooncol 1996;29:223–228.
5. Di RC, Di RA. Meningiomas in childhood. Crit Rev Neurosurg 1999;9:180–188.
6. Erdincler P, Lena G, Sarioglu AC, et al. Intracranial meningiomas in children: review of 29 cases. Surg Neurol 1998;49:136–140.
7. Mehta N, Bhagwati S, Parulekar G. Meningiomas in children: a study of 18 cases. J Pediatr Neurosci 2009;4:61–65.
8. Louis DN, Perry A, Reifenberger G, et al. The 2016 World Health Organization classification of tumors of the central nervous system: a summary. Acta Neuropathol 2016;131:803–820.
9. Germano IM, Edwards MS, Davis RL, et al. Intracranial meningiomas of the first two decades of life. J Neurosurg 1994;80:447–453.
10. Rochat P, Johannesen HH, Gjerris F. Long-term follow up of children with meningiomas in Denmark: 1935 to 1984. J Neurosurg 2004;100:179–182.
11. Brastianos PK, Horowitz PM, Santagata S, et al. Genomic sequencing of meningiomas identifies oncogenic SMO and AKT1 mutations. Nat Genet 2013;45:285–289.
12. Clark VE, Erson-Omay EZ, Serin A, et al. Genomic analysis of non-NF2 meningiomas reveals mutations in TRAF7, KLF4, AKT1, and SMO. Science 2013;339:1077–1080.

13. Zhao JF, Sharma S. Expression of the ROS1 oncogene for tyrosine receptor kinase in adult human meningiomas. Cancer Genet Cytogenet 1995;83:148–154.
14. Robinson DR, Wu YM, Lin SF. The protein tyrosine kinase family of the human genome. Oncogene 2000;19:5548–5557.
15. Takeuchi K, Soda M, Togashi Y, et al. RET, ROS1 and ALK fusions in lung cancer. Nat Med 2012;18:378–381.
16. Charest A, Kheifets V, Park J, et al. Oncogenic targeting of an activated tyrosine kinase to the Golgi apparatus in a glioblastoma. Proc Natl Acad Sci USA 2003;100:916–921.
17. Shaw AT, Ou SH, Bang YJ, et al. Crizotinib in ROS1-rearranged non-small-cell lung cancer. N Engl J Med 2014;371:1963–1971.
18. Ge H, Liu K, Juan T, et al. FusionMap: detecting fusion genes from next-generation sequencing data at base-pair resolution. Bioinformatics 2011;27:1922–1928.
19. Bolstad BM, Irizarry RA, Astrand M, et al. A comparison of normalization methods for high density oligonucleotide array data based on variance and bias. Bioinformatics 2003;19:185–193.
20. Fujita H, Yoshida A, Taniguchi H, et al. Adult-onset inflammatory myofibroblastic tumour of the stomach with a TFG-ROS1 fusion. Histopathology 2015;66:610–612.
21. Lovly CM, Gupta A, Lipson D, et al. Inflammatory myofibroblastic tumors harbor multiple potentially actionable kinase fusions. Cancer Discov 2014;4:889–895.
22. Mordechai O, Postovsky S, Vlodavsky E, et al. Metastatic rhabdoid meningioma with BRAF V600E mutation and good response to personalized therapy: case report and review of the literature. Pediatr Hematol Oncol 2015;32:207–211.
23. Buzyn A, Blay JY, Hoog-Labouret N, et al. Equal access to innovative therapies and precision cancer care. Nat Rev Clin Oncol 2016;13:385–393.